JOURNAL OF GEOPHYSICAL RESEARCH, VOL. 113, D08302, doi:10.1029/2007JD009241, 2008

Sources of particulate matter in the northeastern United States in summer: 2. Evolution of chemical and microphysical properties

C. A. Brock,[1] A. P. Sullivan,[2,3] R. E. Peltier,[2] R. J. Weber,[2] A. Wollny,[1,4] J. A. de Gouw,[1,4] A. M. Middlebrook,[1] E. L. Atlas,[5] A. Stohl,[1,4,6] M. K. Trainer,[1] O. R. Cooper,[1,4] F. C. Fehsenfeld,[1,4] G. J. Frost,[1,4] J. S. Holloway,[1,4] G. Hübler,[1,4] J. A. Neuman,[1,4] T. B. Ryerson,[1] C. Warneke,[1,4] and J. C. Wilson[7]

Received 31 July 2007; revised 9 November 2007; accepted 12 December 2007; published 22 April 2008.

[1] Measurements of aerosol particle size distributions and composition and of trace and reactive gas mixing ratios were made on the NOAA WP-3D aircraft downwind of mixed urban/industrial sources in the northeastern United States (U.S.). These measurements were made in noncloudy air during July and August 2004, under conditions where cloud processing was not likely to play an important role in oxidation chemistry. Under these conditions, particulate sulfate was found to be produced with an exponential time constant of ~3.5 d from the gas-phase oxidation of SO_2, which was ubiquitous but inhomogeneously distributed in the pollution plumes. When submicron particle mass concentrations exceeded 15 μg m^{-3}, sulfate and associated ammonium dominated the composition; at lower mass concentrations particulate organic matter (OM) dominated. Since most of the urban plumes sampled contained substantial SO_2 from nearby industrial sources, the apportionment of aerosol mass between OM and sulfate compounds under noncloudy conditions was governed largely by the differences between the oxidation timescales of SO_2 and those of precursor volatile organic compounds (VOCs) relative to their transport time. These differences in oxidation timescales may explain much of the variability in previously published OM/sulfate ratios for this region. These observations indicate that even with higher-than-expected secondary OM formation, in the northeastern U.S. the potential inorganic particulate mass from SO_2 emissions significantly exceeds the potential secondary OM from anthropogenic VOC emissions.

Citation: Brock, C. A., et al. (2008), Sources of particulate matter in the northeastern United States in summer: 2. Evolution of chemical and microphysical properties, *J. Geophys. Res.*, *113*, D08302, doi:10.1029/2007JD009241.

1. Introduction

[2] Atmospheric aerosol particles are important in a variety of atmospheric processes and properties. They alter the Earth's radiation budget directly and indirectly through their effects on cloud properties and lifetimes, they transport and distribute chemical compounds to the Earth's surface, and they reduce visibility and affect human health [e.g., *McMurry et al.*, 2004]. The size, concentration, composition, and distribution of aerosol particles is highly variable because of short atmospheric lifetimes and widely dispersed and heterogeneous sources [e.g., *Seinfeld and Pandis*, 1998].

[3] Along the northeastern coast of the United States (U.S.) several large metropolitan areas, including Washington D.C., Baltimore, Philadelphia, New York City, and Boston, combine to form a megalopolis of ~40 million inhabitants. Anthropogenic sources of particles and gas-phase particle precursors within this region are dominated by emissions from mobile sources and from coal-fired industries and power generation stations. Many of the SO_2 sources in the northeastern U.S. are small relative to the very large power generation facilities in the Ohio River Valley (Figure 1); however, there are many of them and they are often within or very close to urbanized areas. Consequently, the air affected by emissions from many northeastern U.S. cities contain not only the products typical of a large urban area, such as soot, CO, NOy (the sum of

[1]Earth System Research Laboratory, NOAA, Boulder, Colorado, USA.
[2]School of Earth and Atmospheric Sciences, Georgia Institute of Technology, Atlanta, Georgia, USA.
[3]Now at Department of Atmospheric Science, Colorado State University, Fort Collins, Colorado, USA.
[4]Also at Cooperative Institute for Research in Environmental Sciences, University of Colorado, Boulder, Colorado, USA.
[5]Rosenstiel School of Marine and Atmospheric Science, University of Miami, Miami, Florida, USA.
[6]Also at Norwegian Institute for Air Research, Kjeller, Norway.
[7]Department of Engineering, University of Denver, Denver, Colorado, USA.

0148-0227/08/2007JD009241$09.00

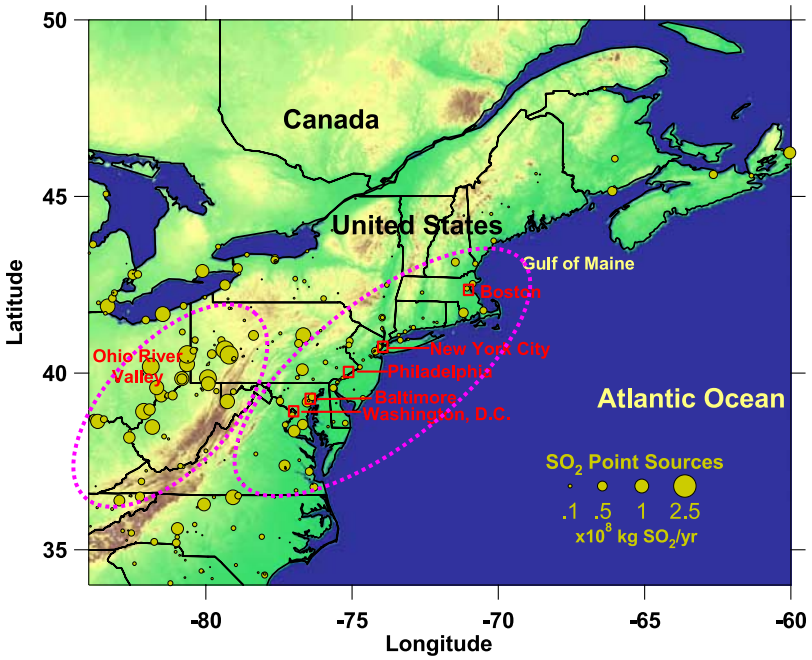

Figure 1. Map of the northeastern United States and southeastern Canada. Circles indicate point sources of SO_2; large urban areas are shown. Almost continuous urban and suburban development extends from Washington, D.C., to Boston. Most large industrial SO_2 sources are in the Ohio River Valley region west of the Appalachian Mountains and did not significantly affect the data selected for this analysis.

reactive nitrogen species), VOCs, and primary and secondary particulate organic matter (OM), but often substantial quantities of SO_2 and sulfate-containing particles. According to a 1999 emission inventory produced by the U.S. Environmental Protection Agency (EPA NEI 1999 V.3 [*United States Environmental Protection Agency* (*U.S. EPA*), 2003]), the SO_2 produced from northeastern U.S. sources (eastern area circled in Figure 1) during the summer season totals $4x10^6$ kg d^{-1}, or about 1/3 of the output of sources in the Ohio River Valley region (western area circled in Figure 1).

[4] The relative importance of the major constituents of particulate matter in this region of the U.S. has been a subject of considerable discussion. In general, sub-2.5 μm particulate mass in the eastern U.S. is composed predominately of sulfate and associated ammonium, and of OM, soot, nitrate, crustal matter, and water [*Malm et al.*, 2004]. Nitrate and soot are most significant in wintertime, when ammonium nitrate is thermodynamically favored and when atmospheric mixing is at a minimum. However throughout the year, sulfate (with ammonium) and OM represent more than 70% of the sub-2.5 μm mass, and an even larger fraction in summertime. Prior to findings from the airborne Tropospheric Aerosol Radiative Forcing Observational Experiment (TARFOX) in summer of 1996 [*Novakov et al.*, 1997; *Hegg et al.*, 1997], sulfate was believed to be the primary contributor to fine particle mass in this region of the country and season. *Hegg et al.* found that on average, OM was present in higher mass concentrations than sulfate and associated ammonium, and that OM dominated the light scattering properties of the aerosol. *Bates et al.* [2005] found similar results that highlighted the importance of OM on the basis of measurements in the summer of 2002 aboard the NOAA research vessel *Ronald H. Brown* in the Gulf of Maine as part of the first New England Air Quality Study (NEAQS). During the second NEAQS shipboard study in 2004, *Quinn et al.* [2006] reported high OM mass fractions close to the city of Boston, with a composition dominated by sulfate species in more aged air masses in the Gulf of Maine. Observations in New York and Philadelphia [*Drewnick et al.*, 2004] show roughly equal contributions to fine particle mass from inorganic and organic compounds.

[5] This paper is part 2 of an analysis of measurements collected on the NOAA WP-3D aircraft during the second New England Air Quality Study/Intercontinental Transport and Chemical Transformations project of 2004, a part of the larger International Consortium for Atmospheric Research on Transport and Transformation (ICARTT) program. In part 1 [*de Gouw et al.*, 2007, hereinafter referred to as part 1], the budget of VOCs and particulate OM are examined to show that OM is predominantly secondary, likely anthropogenic, and photochemically produced with a time constant <1 d, consistent with results from the first NEAQS study in 2002. Here in part 2, we examine the temporal evolution of particle microphysical and chemical properties from the source regions, and find that in most cases, the amount of sulfate + potential sulfate mass from SO_2 exceeds the amount of OM formed within plumes from anthropogenic sources. Furthermore, some of the compositional discrepancies noted in previous studies can be explained by differences in the timescale of formation of OM and secondary aerosol sulfate from gas-phase SO_2 oxidation. Not only are these results significant for U.S. air quality and visibility concerns, but they are also relevant to intercontinental transport and climate change due to the flux of pollutants from North America across the Atlantic

Ocean to the Eurasian continent and to resulting effects upon hemispheric photochemistry and climate forcing [e.g., *Stohl et al.*, 2002; *Akimoto*, 2003; *Li et al.*, 2004; *Parrish et al.*, 2004; *Owen et al.*, 2006].

[6] In this work, we first describe the observational and analytical techniques used. Next, we present a case study that examines the multiday temporal evolution of aerosol plumes from northeastern U.S. sources that were transported above the marine boundary layer with no additional input from surface sources and with no dry or wet deposition or cloud interaction. We then select a larger portion of the entire data set for more quantitative analysis, compare the results with previously published findings, and draw generalized conclusions.

2. Methods

[7] The data analyzed here were collected aboard the NOAA's WP-3D research aircraft which carried a number of instruments for measuring aerosol particle microphysical and chemical properties, the mixing ratios of a number of gas-phase reactive and tracer species, photolysis rates, and cloud microphysics. Methodologies and uncertainties of the measurements and analysis techniques used here are described below. Some data acquired aboard the NOAA research vessel *Ronald H. Brown* (RHB), which operated in the Gulf of Maine and nearby coastal waters, will also be presented. More detailed information regarding measurements on RHB are found in the work of *Bates et al.* [2002, 2005], *Quinn and Bates* [2005] *Quinn et al.* [2006], *Mader et al.* [2003], *de Gouw et al.* [2005, 2007], and *Warneke et al.* [2004, 2005].

2.1. Particle Size Distributions

[8] Particle size distributions were measured with three instruments described below which, coupled with a nonlinear inversion technique, produced particle size distributions from 0.003 to 8.3 μm diameter every second. The analysis presented in this paper will focus on the submicron portion of the size distribution, which vastly dominated the particle number and surface area and which comprised the majority of the particle volume in the measured aerosols. Independent measurements of particle number and volume made on the NOAA WP-3D and the NASA DC-8 were compared during three side-by-side flight legs; these comparisons are available online at http://www.esrl.noaa.gov/csd/ICARTT/fieldoperations/fomc.shtml. The measurements were made in clean and polluted air masses above and within the boundary layer, leading to a large dynamic range in most variables and varying ambient temperatures and pressures. Briefly, the integral measurements of ultrafine number, submicron number and submicron volume agreed within the combined experimental uncertainties in 7 of 9 possible comparisons, and were within two times the stated uncertainties in the remaining cases. Measurements of supermicron particle properties were not compared.

2.1.1. Ultrafine Particles

[9] An instrument composed of five condensation particle counters (CPCs) measured the cumulative particle concentration in five ultrafine (diameter <0.1 μm) size classes, with 50% detection efficiencies at 0.004, 0.008, 0.015, 0.030, and 0.055 μm diameter [*Brock et al.*, 2000]. This instrument operated in an underwing pod sampling air from a double-diffusing inlet that sampled submicron particles with unity efficiency [*Jonsson et al.*, 1995]. The sample flow rate to the instrument was constant at 45 volumetric cm^3 s^{-1}. The sample air was warmed to 35°C prior to detection, reducing the relative humidity (RH) for more than 90% of the samples to <50% RH. Size distributions were derived from the observed concentrations in the five size classes as described in section 2.1.5.

2.1.2. Fine Particles

[10] A modified Lasair 1001 laser optical particle counter (OPC, Particle Measuring Systems Inc., Boulder, CO, USA) measured particle size distributions in 64 size bins over a diameter range from 0.12 to 0.95 μm, with a sample flow rate of 5 volumetric cm^3 s^{-1} from within the same pod using the same inlet. The sample RH was not actively controlled in this instrument, but was measured at the instrument inlet with a humidity sensor (Humitter 100Y, Vaisala Inc., Vantaa, Finland). The 10th, 50th, and 90th percentile values for the sample RH for this instrument were 7, 36, and 52%, respectively, for the data analyzed here. Because the mixed organic/sulfate particles that dominated the number population in this size range were likely hygroscopic, a significant RH correction was applied to the data. The hygroscopic diameter growth of mixed organic/sulfate particles reported in the work by *Santarpia et al.* [2004, Figure 10] was fitted with a function of the form $g(RH) = 1 + 1.786 \times 10^{-8} \times RH^{3.779}$, where g(RH) is the ratio of the diameter of the particle at the given RH (in percent) to that at 0% RH. The diameters of Lasair size bins were corrected from instrument RH (RH_{meas}) to conditions of 40% RH by dividing by a factor of $g(RH_{meas})/g(40\%)$. Note that even at 40% RH, ~6% of the particle volume is attributable to water.

2.1.3. Coarse Particles

[11] A second OPC that uses a white-light-emitting diode as the light source was operated inside the aircraft. This white-light OPC measured particle size distributions from 0.7 to 8.3 μm diameter at a sample flow rate of 67 volumetric cm^3 s^{-1}. The 85 cm sample line between the exit of the LTI and the white-light OPC was heated to maintain the measured sample RH $\leq$ 40%. During flight the instrument exhibited periods of gain instability which were not repeatable during ground-based calibrations, and which were not correlated with any known flight condition such as altitude, ambient temperature, airspeed, or angle of attack. These periods of gain instability were evident by shifts in the size distribution to larger sizes than were reported by the Lasair OPC, without changes in the shape of the size distribution. We have attempted to account for these instrumental shifts by adjusting the gain in the white-light OPC postprocessing software so that the integrated, RH-corrected number concentration reported by the white-light and laser OPCs in the instrumental overlap region between 0.7 and 0.95 μm diameter agrees. These changes do not substantially affect the submicron particle measurements reported here, since in this case "submicron" refers to measurements made downstream of an impactor with a 1.0 μm aerodynamic diameter (~0.75 μm physical diameter, see section 2.1.4).

2.1.4. Low-Turbulence Inlet and Impactor

[12] The white-light optical particle counter (section 2.1.3) and the particle-into-liquid sampler (PILS, section 2.2)

sampled from an airstream decelerated from the aircraft speed of ~100 m s^{-1} to a few m s^{-1}. The University of Denver low-turbulence inlet (LTI [*Huebert et al.*, 2004; *Wilson et al.*, 2004]) produced laminar deceleration of the airstream with calculable effects on particle concentrations. Inertial enhancements of particle concentrations in the LTI were determined from computational fluid dynamics simulations, and are inconsequential for the submicron aerosol that is the focus of this work [*Wilson et al.*, 2004]. Particle losses in the sample line tubing to the downstream instruments were calculated using established parameterizations [*Baron and Willeke*, 2001], and were also negligible for the submicron aerosol.

[13] A PILS and an Aerodyne quadrupole aerosol mass spectrometer (AMS) (section 2.2 and part 1, respectively) were operated downstream of a single-stage micro-orifice uniform deposition impactor (Model 100, MSP Corp., Shoreview, Minnesota, USA) with a nominal 50% cut point at an aerodynamic diameter of 1.0 μm. The physical diameter for 50% impactor efficiency for a particle with a density of 1500 kg m^{-3} was 0.79 μm at the typical sampling pressure of 900 mbar and temperature of 288 K, and varied from 0.72 to 0.81 μm for the data analyzed here. The impactor was coated with Apiezon Type L vacuum grease to reduce coarse particle bounce into the downstream sample line.

2.1.5. Calculation of Particle Size Distributions and Uncertainties

[14] To produce a continuous particle size distribution from the 3 instruments, we used a nonlinear iterative inversion algorithm [*Markowski*, 1988]. The inversion is used primarily to determine the size distribution from the very coarse size resolution of the five-channel CPC, as well as to interpolate between the CPC with the largest nucleation diameter, 0.055 μm, and the minimum detectable diameter of 0.12 μm of the laser OPC. The inputs to the inversion procedure were the 5 cumulative concentrations reported by the five-channel CPC, 11 cumulative concentrations produced by summing different RH-corrected size bins of the laser OPC, and 4 cumulative concentrations from summing different bins from the corrected white-light OPC. The inversion procedure calculated a smooth particle size distribution that was consistent within experimental uncertainty with the instrument responses and with the observed cumulative particle concentrations. The inverted size distribution, rather than the directly measured particle size distribution, was used over the Lasair OPC size range because of the improved counting statistics for the 11 cumulative bins compared to the 64 raw differential bins. All the reported particle concentrations were adjusted to standard conditions of 0°C and 1013 hPa.

[15] Uncertainties in the size distributions and integrated properties are attributable to several sources. Random errors, which affect instrument precision, are primarily due to particle counting statistics, but also include variations in flow rate and pressure. We estimate the effect of random errors by running Monte Carlo simulation of these uncertainties through the numerical inversion and into the final size distribution and integrated parameter products. Since these random errors are associated with particle counting statistics, they vary from sample to sample. It is impractical to run Monte Carlo simulations on each second of flight data; however, representative calculations for different typical cases encountered in the NEAQS/ITCT 2004 project show precision for integrated particle volume ranging from 15 to 25%.

[16] Biases include uncertainties in the diameter of calibration particles and differences in refractive index and particle shape between the calibration particles and ambient particles. The correction for relative humidity made to the Lasair OPC and the gain shift correction for the white-light OPC are also potential sources of bias in these measurements. Sizing uncertainties due to particle refractive index are estimated by calibrating the laser and white-light OPCs for size and concentration using nearly monodisperse particles with compositions ranging from dioctyl sebacate to polystyrene latex, which span the range of likely refractive indices for nonabsorbing atmospheric particles. The primary calibration standard used was ammonium sulfate, and size distributions from the optical particle counters are referenced to this composition. The uncertainty in the RH correction was estimated from the variability in the atmospheric data on hygroscopic properties of mixed organic sulfate particles presented by *Santarpia et al.* [2004]. Total estimated biases from the above sources, propagated through the data processing algorithms by Monte Carlo simulation, are <15%, <28%, and <38% for integrated particle number, surface and volume concentrations, respectively. These calculated biases do not include the effects particle shape, highly absorbing components such as soot, or particle volatility at sampling temperatures as high as 35°C. Biases from these sources are likely <10% given the mixed organic-sulfate composition of the particles and the small mass contribution from soot [*Clarke et al.*, 2007].

2.2. Particle-Into-Liquid Sampler

[17] The composition of submicron particles was measured with a particle-into-liquid sampler (PILS) with two online detectors to measure inorganic ionic constituents by ion chromatography (IC [*Orsini et al.*, 2003]) and water soluble organic carbon (WSOC) by an aqueous carbon detector [*Sullivan et al.*, 2006]. The PILS operated within the aircraft fuselage and sampled air from the University of Denver LTI and the impactor. Denuders between the impactor and the saturator removed gas-phase SO_2, NH_3, HNO_3, and organic gases prior to condensation and droplet collection. Biases due to particle enhancement or inertial loss were calculated to be negligible for the submicron particles sampled by the PILS. The PILS-IC measured the inorganic ions sulfate, nitrate, chloride, ammonium, calcium, potassium, magnesium, and sodium with a collection time of 1.5 min and a sample period of 2.45 min. Detection limits for these components were 0.02–0.5 μg m^{-3}, and precision was ~20%. Comparison of sulfate measurements made by the WP-3D PILS-IC and one operated on the NASA DC-8 during two side-by-side flight legs (http://www.esrl.noaa.gov/csd/ICARTT/fieldoperations/fomc.shtml) do not show agreement within stated uncertainties, with the DC-8 PILS generally biased low by ~40% compared to the WP-3D PILS and other independent measurements.

[18] The PILS-WSOC measurement used a continuous, inline aqueous organic carbon detector (Model 800 Turbo, Sievers Instruments, Boulder, Colorado, USA) to provide

the water-soluble fraction of submicron organic carbon (WSOC) with a time resolution of ~1 min, and a combined uncertainty of ±(8% + 0.3 μg C $m^{-3}_{(air)}$). The WSOC concentration is a subset of the total submicron particulate organic mass (OM), and its speciation has been examined for urban environments by *Sullivan et al.* [2006] and *Sullivan and Weber* [2006a, 2006b]. The relationship between WSOC and OM is evaluated in part 1. For the remainder of this analysis, OM is estimated from the PILS-WSOC measurements as

$$OM_{calc} = WSOC \times 2.8^{+0.8}_{-1.0}. \quad (1)$$

2.3. VOCs and Reactive Gases

[19] Measurements of volatile organic compounds (VOCs) are described in part 1. In this analysis, we make use of acetonitrile, a sensitive and specific tracer of biomass and/or biofuel burning, which has a long atmospheric lifetime and no significant sinks relevant to this analysis [*de Gouw et al.*, 2003, 2006]. We also use measurements of toluene and benzene, which in this region are emitted primarily from motor vehicles, and which are used to calculate a photochemical lifetime of a polluted air parcel as described in part 1. In addition, the NOAA WP-3D aircraft carried an extensive suite of instruments for measuring the reactive chemistry of primary and secondary pollutants. The subset of these measurements used here (and an associated primary reference, measurement interval, detection limit, and accuracy) included SO_2 (1 s, 600 pptv, 15% [*Ryerson et al.*, 1998]), CO (1 s, 1.7 ppbv, 5% [*Holloway et al.*, 2000]), NO (1 s, 20 pptv, 10% [*Ryerson et al.*, 2000]), NO_2 (1 s, 150 pptv, 10% [*Ryerson et al.*, 2000]), HNO_3 (1 s, 50 pptv, 15% [*Neuman et al.*, 2002, 2006]), peroxyacetylnitrate and related compounds (PANs [*Slusher et al.*, 2004], 2s, 1 pptv, 10%), and O_3 (1 s, 100 pptv, 3% [*Ryerson et al.*, 2000]). Because of instrument difficulties, total reactive nitrogen, NO_y was not directly measured but was calculated from the sum of discretely measured NO, NO_2, HNO_3, and PANs [*Neuman et al.*, 2006]. A detailed comparison of these species independently measured on the NASA DC-8 and the NOAA WP-3D during three separate side-by-side flight legs is available at http://www.esrl.noaa.gov/csd/ICARTT/fieldoperations/fomc.shtml. These gas-phase measurements, together with meteorological parameters provided by the NOAA Aircraft Operations Center (AOC) and the aforementioned VOC and particle measurements, allow in most cases accurate determination of the influence of urban, industrial, agricultural, biogenic, and biomass burning sources on the air being sampled.

2.4. Evaluation of Aerosol Composition Measurements

[20] The performance of the instruments for measuring the composition of submicron particles is critical to the analysis presented in this work. The proxy OM_{calc} and the PILS inorganic compositional data may be compared to the particle volume measurements calculated from the particle size distributions. Particle mass was calculated from measured particle volume assuming a particle density derived from the PILS compositional measurements. The use of the PILS data to calculate particle density means that the two data sets being compared are not completely independent; however, gross errors in particle composition measurements, particularly in the OM_{calc} estimate, should produce systematic biases as composition varies from low to high organic fraction. The volume-weighted mean density, ρ_{calc}, is

$$\rho_{calc} = \frac{OM_{calc} + \sum ion + 0.06 \times V_{fine}}{\left(\frac{OM_{calc}}{\rho_{om}}\right) + \frac{\sum ion}{\rho_{ion}} + \frac{0.06 \times V_{fine}}{\rho_{H2O}}}, \quad (2)$$

where $\sum ion$ is the sum of the inorganic ionic species measured by the PILS-IC, V_{fine} (in units of μm^3 cm^{-3}) is the particle volume calculated from the size distributions measured downstream of the impactor, and ρ_{OM}, ρ_{ion}, and ρ_{H2O} are the densities of the organic species (assumed to be 1.2×10^3 kg m^{-3} [*Turpin and Lim*, 2001]), the inorganic species (assumed to be that of ammonium sulfate, 1.77×10^3 kg m^{-3}), and water (10^3 kg m^{-3}), respectively. Water is assumed to compose 6% of the particle volume at the relative humidity of 40%, on the basis of a fit to hygroscopicity data in a polluted southern U.S. environment [*Santarpia et al.*, 2004]. The mass concentration estimated from the particle volume measurements is then

$$M_{est} = V_{fine} \times \rho_{calc}, \quad (3)$$

in units of μg m^{-3}.

[21] Because the calibration aerosol was ammonium sulfate (dry visible refractive index of ~1.46), and since the refractive index of the organic component was not known but is expected to range from ~1.4 to 1.55 [*Kanakidou et al.*, 2005], no adjustments to account for varying particle refractive index were made. (Mie scattering simulations of instrument response produce a variation in submicron particle diameter of ~10% for this range in refractive index.) At a measurement humidity of 40%, and using OM_{calc} (equation (1)), the submicron particle mass from PILS is linearly correlated ($r^2 = 0.88$) with M_{est} (Figure 2). The agreement between the PILS mass and M_{est} is within the combined experimental uncertainties of the techniques; however, M_{est} appears to be biased high by a factor of ~1.25 over the entire range of observed concentrations and compositions. There is no apparent change in this relationship even at values of acetonitrile >500 pptv (Figure 3), which are associated with biomass burning plumes and OM_{calc} mass fractions >0.9. *Peltier et al.* [2007] find that the discrepancy between the volume-derived submicron mass and the PILS measurements may be resolved by assuming 8% of the volume is unmeasured or insoluble material (i.e., soot and dust), and that the conversion factor between OM/WSOC ratio is 3.1, rather than the 2.8 used here. However, the discrepancy between the measured mass from PILS and M_{est} is within the combined uncertainties of the measurements using either value for OM/WSOC.

3. Observations

[22] In this section we first describe how data were chosen so that the temporal evolution of particle microphysical and chemical properties downwind of U.S. East

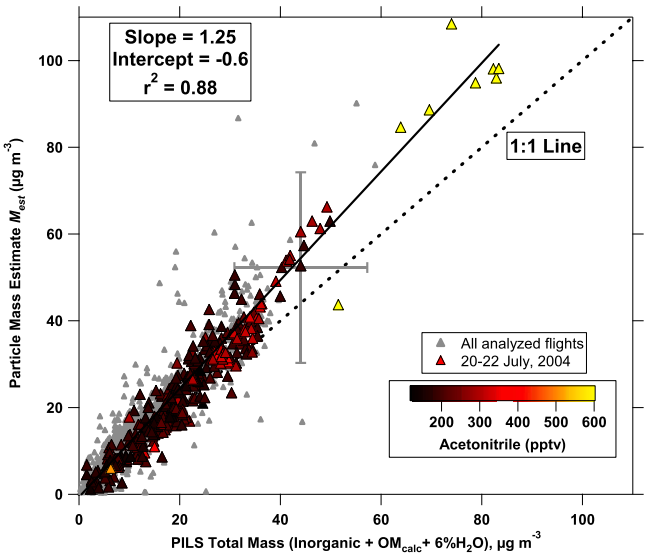

Figure 2. Submicron particle mass calculated from measured particle size distributions using equations (1)–(3), plotted as a function of the sum of particle composition measurements from the PILS instruments. Grey symbols are all the data analyzed in this paper; symbols colored by acetonitrile mixing ratios are a subset of the data from 20 to 22 July as described in section 3.2 (but including high-acetonitrile cases). Solid line is a two-sided least squares linear regression to all the analyzed data; error bars indicate representative uncertainties in the measurements.

Coast urban and industrial sources could be evaluated. We then provide a case study of a multiday transport event to examine in detail how the aerosol evolved. The findings are expanded and generalized in section 4.

3.1. Selection of Data

[23] The observations reported here are a subset of the NEAQS/ITCT 2004 data collected aboard the NOAA WP-3D, which was based in Portsmouth, New Hampshire, for the duration of the program. These data (Table 1) were chosen for analysis because they (1) were collected in air masses generally downwind of major urban and mixed urban/industrial sources along the U.S. East Coast but without substantial contributions from the Ohio River Valley region (Figure 1), (2) included plumes representing a variety of levels of photochemical processing from these sources, and (3) were collected when critical instruments were functioning. Data acquired when acetonitrile mixing ratios exceeded 250 pptv, which are associated with the large biomass burning events in western Canada and interior Alaska that occurred during this period, were excluded from this analysis with the following exception: measurements in the fresh urban plume of NYC on 20 July 2004 included some data with acetonitrile between 250 and 300 pptv (possibly from biofuel sources in the NYC area) which were retained for analysis. Note that the selected data set includes not just periods in urban and industrial plumes, but also periods in the lower free troposphere and in relatively unpolluted rural terrestrial boundary layer air. The selected data are from 7 of the 18 total flights made during the NEAQS/ITCT 2004 mission (Table 1).

[24] Four of the 7 selected flights (on 15, 25, and 31 July and 7 August 2004) include data measured mostly in the continental planetary boundary layer (PBL). In these cases, the targeted urban and industrial plumes may have advected over small point and area sources that added fresh emissions to the more aged primary plumes. We have not attempted to correct for such specific instances, but have instead limited the analysis to periods of flight in which pollutant concentrations within the primary plumes were much larger than the expected contribution from the smaller sources. In addition, as described in section 4.1, backgrounds were subtracted

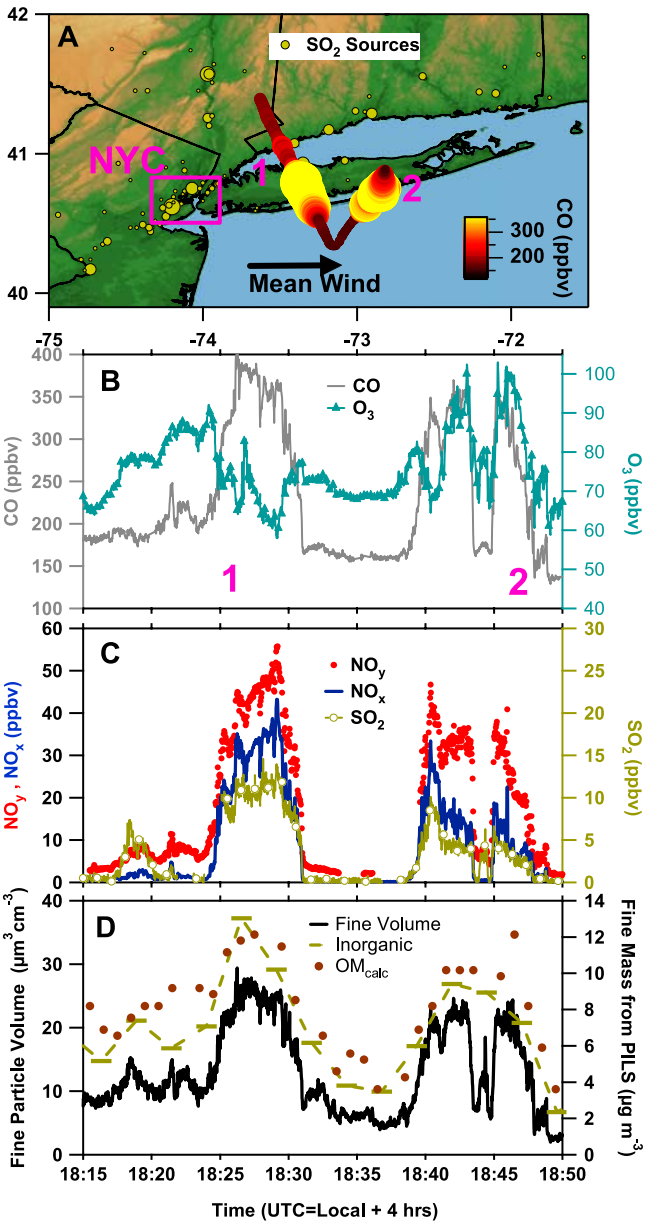

Figure 3. (a) Map showing the location of the WP-3D aircraft on 20 July 2004, color and size coded by CO mixing ratio. Points labeled "1" and "2" are referenced in Figure 3b. (b) Mixing ratios of CO and O_3 as a function of time during the period shown in Figure 3a. (c) Mixing ratios of NO_y and NO_x (left axis) and SO_2 (right axis). (d) Submicron particle volume (left axis), concentration of PILS inorganic species and OM_{calc} (right axis).

Table 1. Flight Dates and Periods Used for Analysis[a]

Date (2004)	Time Periods Included in Analysis, UTC	Region Studied	Light Conditions	Comments
15 Jul	1818–2110	New Jersey–Massachusetts	daylight	strong southwesterly winds; fresh and oxidized NYC plumes; eastern portion of flight over Atlantic excluded because of possible Ohio River Valley influence
20 Jul	1411–1702; 1809–2213	New Jersey–New Hampshire	daylight	southwesterly winds; fresh NYC plumes (Figure 4)
21 Jul	1402–1950	western North Atlantic–Nova Scotia	daylight	southwesterly winds; partially to fully oxidized northeastern U.S. plumes
22 Jul	1508–1927	Gulf of Maine–Nova Scotia–Maine	daylight	southerly winds; aged northeastern U.S. plumes
25 Jul	1415–1735; 1920–2020	Virginia-Massachusetts	daylight	light easterly southeasterly winds; fresh NYC and Boston plumes; western portions of transects excluded to avoid local power plant emissions and clouds
31 Jul	2309–0149; 0203–0241; 0254–0358; 0431–0515	Connecticut-Maine	evening-night	strong southwesterly winds, unoxidized NYC and Boston plumes; western portions of flight excluded because of Ohio River Valley influence
7 Aug	2153–0435	Maryland–Gulf of Maine	evening- night	light westerly winds; fresh, unoxidized NYC and Boston plumes; titrated ozone

[a]Portions of flight affected by biomass burning and fresh point source plumes were also excluded from analysis (see text).

from the analyzed measurements to partially compensate for these regional contributions.

[25] During the other three selected flights (on 20, 21, and 22 July) plumes from urban and industrial East Coast sources were transported to the northeast over the western Atlantic Ocean toward the Canadian Atlantic maritime provinces. A detailed analysis of the evolution of the nitrogen budget within these plumes has been published [*Neuman et al.*, 2006]. Neuman et al. demonstrate that the pollution was transported in stratified layers at altitudes from 160 m to ~2 km. Despite these low altitudes, the plumes were completely isolated from interactions with the extremely shallow marine boundary layer in this region [*Angevine et al.*, 2006] (with the exception of some contact with the land surface of Nova Scotia during portions of the 22 July flight). Neuman et al. show that oxygenated nitrogen species, which are readily lost by dry deposition to the ocean surface, were conserved relative to CO, which has a negligible deposition rate, confirming the lack of interaction between the ocean surface and the pollution layers above. Aerosol constituents attributable to sea salt, such as bromine, chlorine, and sodium, were consistently below detection limits. The measurements reported here were made in cloud-free air, and since the plumes did not undergo significant lifting between the source region and the point of measurement, it is unlikely that clouds were present at any point of the transport. This interpretation is also supported by the conservation of water soluble species as detailed in the work of *Neuman et al.* [2006].

[26] In section 3.2 we examine the multiday evolution of the aerosol characteristics within some of the East Coast urban plumes encountered on these 3 d. Note that this not a true Lagrangian evaluation, since the same air mass may not have been sampled on consecutive days. Furthermore, it is not possible to unequivocally identify the plumes from even large urban sources such as New York City (NYC) more than 1 d downwind, because of the multitude of sources and the complexity of the vertically sheared, laminar transport in the free troposphere. In section 4, we show that the data collected from 20 to 22 July are representative of the larger data set, which is based on sampling a large number of individual plumes from various East Coast sources.

3.2. Temporal Evolution of Urban/Industrial Plumes

[27] Particle composition and size distributions for a fresh, a moderately aged, and a highly aged plume from mixed urban and industrial sources in the eastern U.S. are described in this section. Additionally, tracer mixing ratios and the relationship between pollutants in these plumes are examined. On 20, 21, and 22 July, steady winds advected the plumes from the Boston-Washington urban centers over the northwest Atlantic Ocean and then northward over Nova Scotia, Canada. These cases are suitable for examining the 3-d evolution of plumes from generic urban and industrial sources in the northeastern U.S. in the absence of confounding sources or sinks.

[28] The temporal evolution of these plumes demonstrates five significant features which will be further discussed in section 4: (1) particle sized distributions evolved within 1 d to be dominated by an accumulation mode; (2) OM_{calc} and sulfate (and associated ammonium) were the dominant components of the submicron aerosol composition; (3) the plumes were spatially and chemically heterogeneous, but usually contained substantial amounts of SO_2; (4) OM_{calc} increased relative to CO during the transport (see part 1); and (5) sulfate increased relative to OM_{calc} during the transport.

3.2.1. Fresh New York City Plume

[29] On 20 July 2004, the plume from NYC was intercepted at two locations downwind over and near Long Island, New York (Figure 3). The aircraft was at an altitude of 1.1 km, except for a brief descent to 200 m at 1844 UTC in middle of the second plume, followed by a climb to higher altitude, to probe the vertical distribution of the plume. Maximum mixing ratios of CO exceeded 400 ppbv, SO_2 14 ppbv, and NO_y 50 ppbv in the plume transect closest to NYC (marked "1" in Figure 3), approximately 60 km from the city center. This distance is about 3 times the width of the densely populated city center, and represents approximately 3–4 h advection time given the winds measured aboard the aircraft. More than two thirds of the NO_y present in this plume was in the form of NO_x, and O_3 was titrated by NO to values below the surrounding air (Table 2).

Table 2. Gas-Phase and Aerosol Properties in Plumes From New York City (Two Plumes on Tuesday, 20 July 2004) and From Northeastern U.S. Urban and Industrial Sources (21 July 2004 and 22 July 2004)[a]

Date (2004)	Time, UTC	Distance to NYC, km	Estimated Age, h	Mean CO, ppbv	Mean O_3, ppbv	Mean SO_2, ppbv	Mean NO_x/NO_y	Submicron N, cm^{-3}	Submicron Surface, $\mu m^2\ cm^{-3}$	ΣPILS,[b] $\mu g\ m^{-3}$	Inorg. Fract.[c]	Org. Fract.[d]	$SO_4^=$/Total S	Charge Balance, $\mu eq\ m^{-3}$
20 Jul	1815–1820	NA[e]	NA	185	73	2.2	0.24 ± 0.08	1.5×10^4	290	12^{+3}_{-1}	$0.50^{+0.18}_{-0.15}$	$0.50^{+0.15}_{-0.18}$	0.30 ± 0.10	0.015 ± 0.008
20 Jul	1826–1829	60	3.5	368	68	10.9	0.72 ± 0.23	2.9×10^4	760	24^{+6}_{-2}	$0.55^{+0.06}_{-0.24}$	$0.45^{+0.24}_{-0.06}$	0.12 ± 0.03	0.030 ± 0.007
20 Jul	1840–1843	100	4.3	327	81	5.5	0.54 ± 0.18	1.8×10^4	560	20^{+5}_{-2}	$0.55^{+0.07}_{-0.25}$	$0.45^{+0.25}_{-0.07}$	0.22 ± 0.06	0.069 ± 0.005
21 Jul	1515–1526	570	40	283	132	4.7	0.04 ± 0.01	8.4×10^3	570	34^{+8}_{-4}	$0.58^{+0.07}_{-0.22}$	$0.42^{+0.22}_{-0.07}$	0.41 ± 0.11	−0.052 ± 0.010
22 Jul	1605–1612	900	80	195	83	3.2	0.015 ± 0.003	3.4×10^3	520	27^{+5}_{-3}	$0.77^{+0.07}_{-0.19}$	$0.23^{+0.19}_{-0.07}$	0.56 ± 0.15	NA[f]

[a]Error bounds for calculated values are propagated instrument uncertainties. Errors for directly measured values given in section 2.
[b]Sum of inorganic species measured by PILS-IC + assumed water + OM_{calc}.
[c]Inorganic fraction. Sum of inorganic species measured by PILS-IC + assumed water divided by sum of inorganic species, water, and OM_{calc}. Ammonium was not measured on 22 July 2004 and is estimated assuming a composition of $(NH_4)HSO_4$.
[d]Organic fraction. OM_{calc} divided by sum of inorganic species, assumed water, and OM_{calc}. Ammonium was not measured on 22 July 2004 and is estimated assuming a composition of $(NH_4)HSO_4$.
[e]NA, not applicable. This sample is a background case adjacent to the fresh NYC plume.
[f]NA, not applicable. Cations not measured on this flight.

[30] The ratio of total sulfur (gas-phase SO_2 + particulate sulfate in ppbv) to NO_y, derived from the slope of the linear least squares regression between these variables, was 0.29. This ratio is consistent with the NYC urban area ozone-season gridded emissions inventory (EPA NEI 1999 Version 3) molar ratio of SO_2/NO_x of 0.25. Approximately 45% of the inventoried SO_2 comes from the several industrial and power generation point sources in the NYC metropolitan area, while 42% originates from nonmobile area sources. (Note that the largest of the SO_2 point sources in this region are located in the southwest portion of the NYC urban area. The wind direction at the time of measurement resulted in the SO_2 emissions being superimposed upon the strong NYC urban signature.) The second transect of the NYC plume, which was made approximately 100 km (4–5 h transit time) downwind of the city center, had slightly lower concentrations of primary pollutants and was more photochemically aged, with mean NO_x/NO_y ratios near 0.5.

[31] Submicron particulate volume, inorganic mass, and OM_{calc} were correlated with the gas-phase primary pollutants in both plume transects. Within both transects, the inorganic particulate mass almost doubled relative to background values (Table 2). The composition of the particles measured by the PILS between 1825 and 1829 UTC, over which interval the mean CO mixing ratio was 373 ppbv in the center of the first NYC plume transect, was dominated by ammonium, sulfate, and organics (Figure 4). The composition averaged over comparable conditions during the second transect was very similar. The charge balance of the measured inorganic ionic species was positive (Table 2) [*Peltier et al.*, 2007].

[32] Particle size distributions (Figure 4) were averaged across the first transect downwind of NYC where CO exceeded 300 ppbv and across the second transect of the NYC plume where CO exceeded 300 ppbv and O_3 exceeded 80 ppbv (i.e., in the more photochemically processed portion of the plume). In both transects, number concentrations were dominated by an Aitken mode with a peak diameter near 0.08 μm, with a main volume peak near 0.4 μm and a coarse mode volume peak near 6 μm. Particle number concentrations within the first plume transect were higher than background concentrations by almost a factor of two, while concentrations were a factor of 1.2 times greater than background values in the second, more oxidized and aged transect (Table 2).

3.2.2. Moderately Aged Baltimore–New York City Plume

[33] On 21 July, multiple layered plumes were intercepted southeast and east of Cape Cod, Massachusetts. Carbon monoxide, O_3, SO_2, NO_y, V_{fine}, and OM_{calc} were enhanced above background (Figure 5). Plumes of similar source, age, and chemical characteristics were also observed on 20 July in the same area. The NO_x/NO_y ratio was 0.04 (Table 2), indicating that the plume was significantly oxidized. The particulate components were positively correlated with the gas-phase pollutants in the plumes; however the plumes were not spatially or chemically homogeneous. This heterogeneous spatial and chemical nature suggests that a variety of sources that were not fully mixed together contributed to the polluted layers. The FLEXPART transport model [*Stohl et al.*, 2002, 2003] was used to calculate source contribution maps for North American emissions,

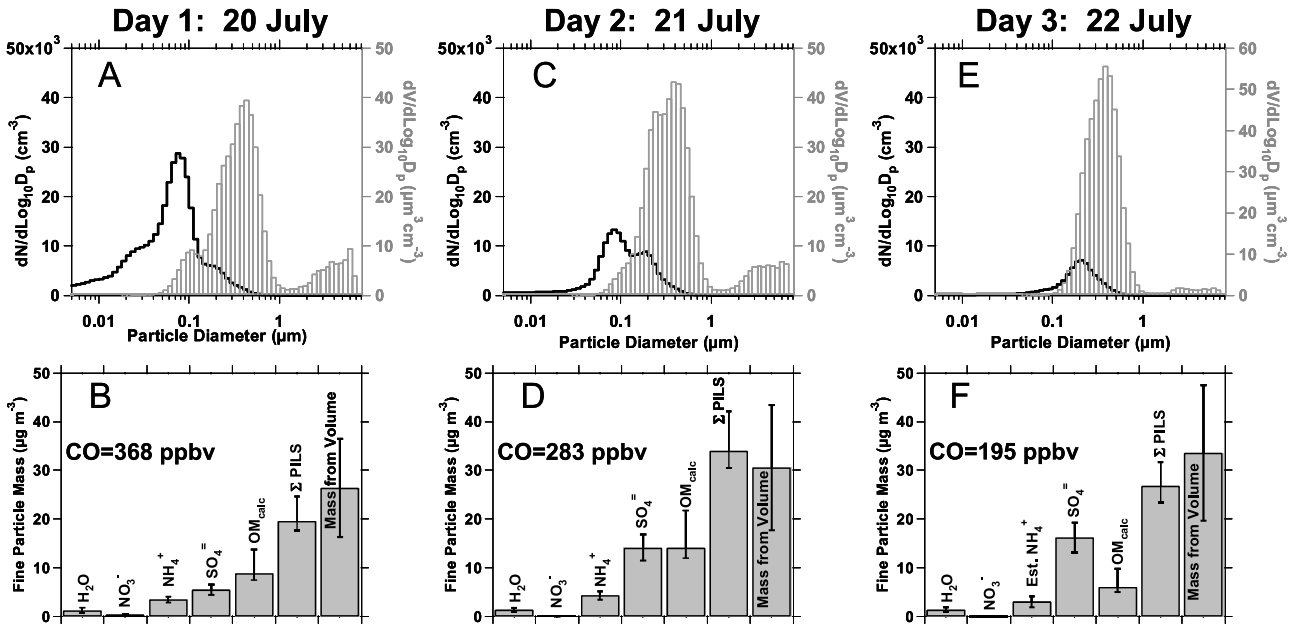

Figure 4. (a) Particle number (line, left axis) and volume (bars, right axis) size distributions measured on 20 July 2004 in the first transect marked "1" in Figure 3 when CO exceeded 300 ppbv. (b) Submicron particle composition from the PILS inorganic measurements and OM_{calc} during this time interval. (c and d) As in Figures 4a and 4b but measured between 1515 and 1526 UTC on 21 July 2004 as shown in Figure 5. (e and f) As in Figures 4a and 4b but measured between 1603 and1614 UTC on 22 July. CO concentrations are provided as a proxy for dilution.

and indicates that sources of CO ranging from the NYC to Baltimore/Washington D.C. urban regions contributed to the observed layers [*de Gouw et al.*, 2007]. The transport time from these CO sources to the location of the aircraft was ~40 h. The FLEXPART model excludes anthropogenic sources in the Ohio River Valley industrial region (Figure 1) as being significant direct contributors to the plumes that were rich in CO. However, the FLEXPART simulations also suggest that anthropogenic emissions of SO_2 from some of the large point sources in the Ohio River Valley may have contributed to a minor portion of the elevated concentrations of SO_2 and sulfate. Several large SO_2 point sources outside of the urban centers in the Baltimore and Washington area are the most likely sources of the elevated SO_2 that is not well correlated with CO.

[34] Particle size distributions and composition were measured during a section of flight when mean CO was 283 ppbv (Figures 4c and 4d). The particle number distribution (Figure 4c) yields concentrations a factor of 3.5 lower than in the NYC plume observed the previous day (Figure 4a). The fraction of particles with diameters <0.1 μm was lower on 21 July compared with 20 July, and the mass mean diameter was again near 0.4 μm.

[35] The composition of the particles measured by the PILS during this interval on 21 July (Figure 4d and Table 2) was, as in the fresher NYC plume observed the previous day, dominated by ammonium, sulfate, and organics. Nitrate was not present in detectable concentrations, and the inorganic components, ammonium and sulfate, were a larger fraction of the total fine mass than in the fresher NYC plume (Figure 4b). The fraction of total sulfur that was present as particulate sulfate was almost twice that on the previous day, and the charge balance of the measured inorganic ionic components was significantly negative, implying an acidic aerosol. The SO_2 remaining in the plume, almost 5 ppbv, would produce ~19 μg m^{-3} of additional sulfate if fully oxidized.

[36] Over the width of the transect across the polluted region, the relative contribution of organics and inorganic matter to the total aerosol mass varied. In general, where CO concentrations were highest, indicating a large urban contribution, OM_{calc} and inorganic matter contributed approximately equally to submicron particle mass. Where SO_2 was present and CO <250 ppbv, inorganic matter, mostly partially neutralized sulfate, dominated the particle composition.

3.2.3. Highly Aged U.S. East Coast Plume

[37] On 22 July, as on the previous day, the WP-3D encountered a broad region containing layers of polluted air originating from the urban corridor along the U.S. east coast (Figure 6). This region of polluted air extended beyond 47.5°N, north of Nova Scotia and Prince Edward Island, Canada. This analysis focuses on layers of photochemically aged pollution observed in the Bay of Fundy region between southern Nova Scotia and the continent, between sections marked "5" and "6" in Figure 6. In this region, mixing ratios of CO exceeded 250 ppbv and averaged 195 ppbv, compared with values outside of the plumes of ~150 ppbv. Cations were not measured during this flight, so to estimate total particulate mass ammonium was assumed to be present with a 1:1 molar ratio relative to sulfate (i.e., a composition of $(NH_4)HSO_4$).

[38] Submicron inorganic aerosol mass exceeded 25 μg m^{-3}, and was positively correlated with the SO_2 in

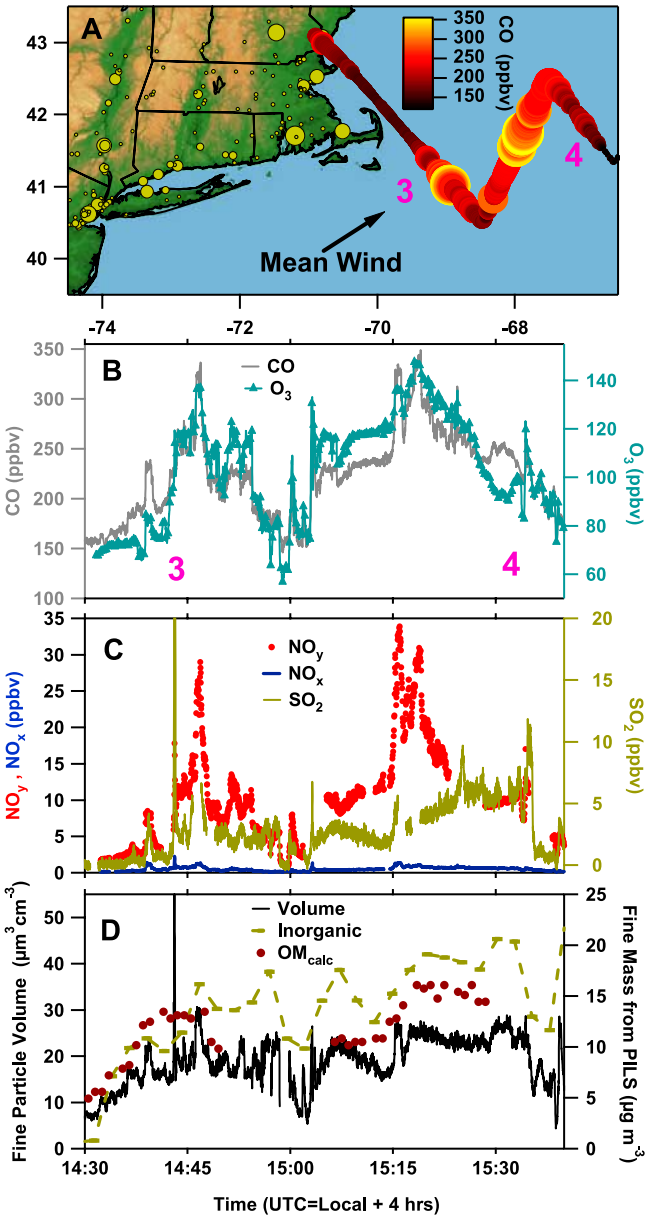

Figure 5. (a–d) As for Figure 3 but measured on 21 July 2004 in a more aged plume about 2 d since emission. Points labeled "3" and "4" in Figure 5a are shown for reference in Figure 5b.

the plumes. In general in this time period, NO_y, O_3, and CO were positively correlated, and SO_2, particle volume, and inorganic mass were positively correlated, but these two groups of pollutants were not well correlated with each other (Figure 6), indicating poorly mixed contributions from multiple sources.

[39] The exact sources of the polluted air are not known. The FLEXPART model again indicates that urban CO sources from the heavily populated U.S. east coast produced the layers, and that industrial sources in the Ohio River Valley were not important contributors to the observed pollution. Values of $NO_x/NO_y < 0.03$ indicate that the pollution was photochemically well aged, and that anthropogenic emissions from small, nearby sources in southern Nova Scotia could not have contributed to the layers encountered during this portion of the flight.

[40] Particle size distributions and composition during this period (Figure 4e and Table 2) yield number concentrations a factor of 8.5 lower than in the fresh NYC plume observed 2 d prior (Figure 4a). Only an accumulation mode, with a number mean diameter near 0.2 μm, was present in the submicron portion of the distribution, and the volume median diameter was ~0.4 μm. The submicron particle composition was dominated by inorganic species. Particulate nitrate was not present above detection limits during this portion of the flight. More than half of the sulfur measured within the polluted region was in the form of aerosol sulfate (Table 2), and sulfate concentration exceeded

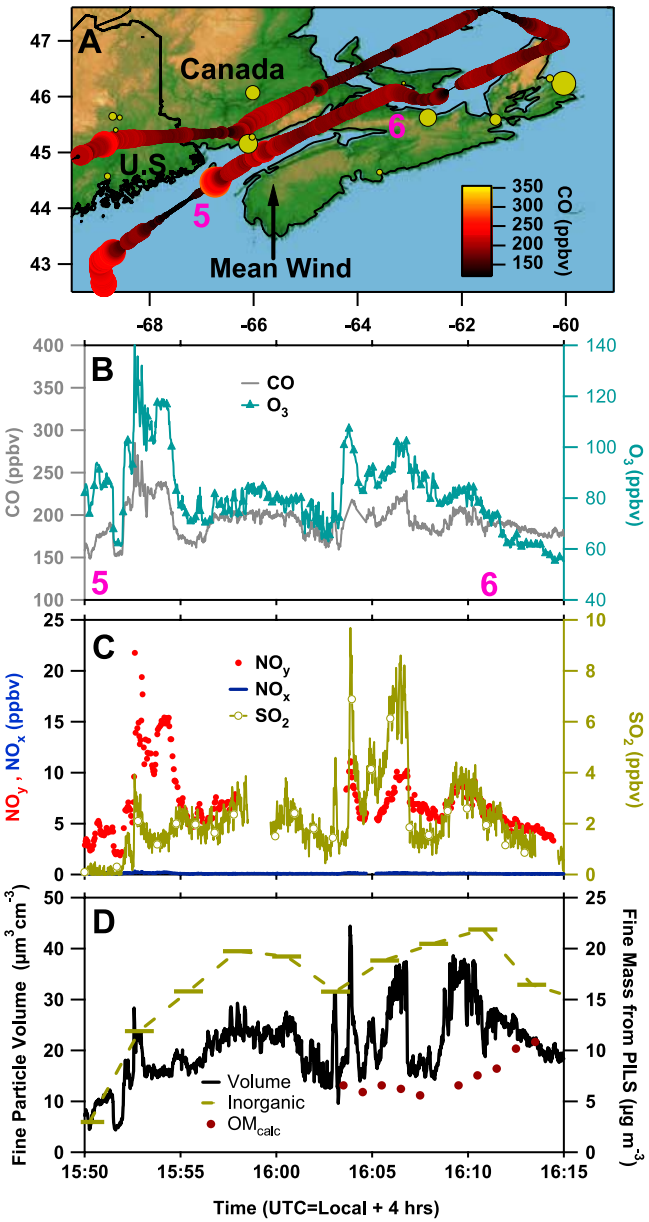

Figure 6. (a–d) As for Figure 3 but measured on 22 July 2004 in a more aged plume about 3–4 d since emission. Points labeled "5" and "6" in Figure 6a are shown for reference in Figure 6b.

15 μg m^{-3}. These values are similar to those reported by *Daum et al.* [1996] in measurements made in similarly aged pollution plumes found southeast of Nova Scotia. Because cations were not measured, the charge balance could not be calculated. However, in many other flights in this data set, *Peltier et al.* [2007] noted a significant deficit of ammonium relative to anions in similar plumes with large mass fractions of sulfate relative to OM_{calc}.

[41] The coarse mode was not a substantial contributor to particle volume in this aged, polluted layer, possibly because of gravitational settling. (Note that the settling velocity of a 5 μm spherical particle with a density of 2000 kg m^{-3} is ~130 m/d, and the layer was observed between 300 and 800 m above sea level.)

4. Analysis

[42] The complexity and diversity of the polluted layers detected during this multiday transport period between 20 and 22 of July are a result of the spatial, temporal, and chemical variation of emissions from the many industrial and urban sources present along the eastern coast of the U.S., as well as of atmospheric chemistry and meteorology during transport. In this section we analyze observations made throughout the NEAQS/ITCT project, in addition to those on 20–22 July. These data were filtered against biomass burning and altitude as indicated in section 3.1, and include periods of transport over land as well as ocean, and nighttime as well as daytime. We draw broad conclusions from these observations, recognizing that specific individual cases, times, and locations may produce results that differ substantially from those of the ensemble of observations reported here.

[43] In part 1, we showed that most of the OM_{calc} in mixed urban/industrial plumes in the northeastern U.S. was secondary and associated with anthropogenic emissions. The timescale for the secondary OM_{calc} production was observed to be <1 d. In this section, we examine evidence for the secondary formation of sulfate from gas-phase oxidation of SO_2, and compare these results with the magnitude and rate of particulate OM_{calc} production as reported in part 1.

4.1. Sulfate Dominates Submicron Particulate Mass at High Loadings

[44] In section 3, the chemical composition of submicron particles in plumes from cities in the northeastern U.S. was examined in detail. In the few-hours-old plume from NYC measured on 20 July, sulfate and associated ammonium contributed about 55% of the mass. In the day-old plumes from the region near NYC measured the following day, sulfate and ammonium combined were 58% of the mass, and in older plumes from east coast cities measured a day later, on 22 July, sulfate and (estimated) ammonium represented 77% of the total mass. *Quinn et al.* [2006] analyze the 2004 RHB AMS observations and report similar increases in the relative contribution of sulfate compounds with increasing distance from the U.S. east coast.

[45] The source of the increased proportion of sulfate in the submicron particulate mass budget was oxidation of SO_2 to form particulate sulfate. The fraction of total plume sulfur (particulate sulfate + gas-phase SO_2) that was present as particulate sulfate increased with increasing plume age and oxidation (Figure 7). The particulate ammonium originated from gas-phase ammonia, which quickly partitions to the particle phase when excess sulfate is present. Since ammonia was not added to the plumes as they were transported above the MBL, once the ammonia was consumed, the aerosol composition should have become increasingly dominated by anions as sulfate mass was added [*Peltier et al.*, 2007]. The ion balance measured on 21 July was indeed significantly more negative compared to that on 20 July (Table 2; no ammonium measurements were available on 22 July).

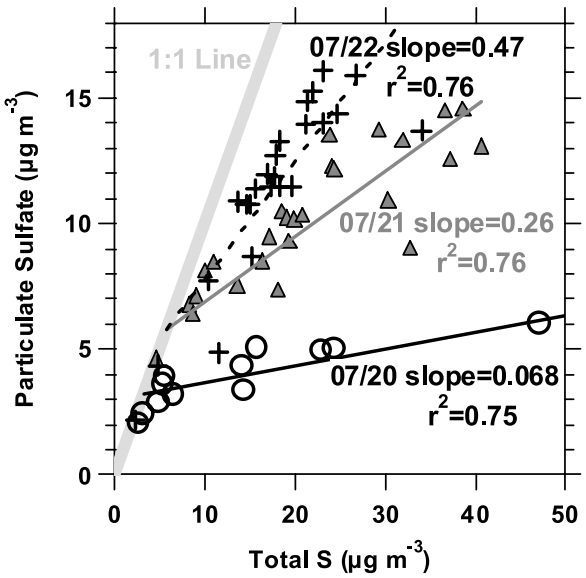

Figure 7. Particulate sulfate plotted as a function of total sulfate (particulate sulfate + SO_2 as sulfate in μg m^{-3}) measured on 20, 21, and 22 July 2004 in urban plumes during the periods shown in Figures 3, 5, and 7, respectively.

[46] As noted earlier, there are a large number SO_2 point sources located throughout the east coast urban corridor (Figure 1). The cumulative significance of these sources is evident in the pervasive presence of elevated mixing ratios of SO_2, often exceeding 5 ppbv, found in the plumes encountered on 21 and 22 July over the western Atlantic Ocean, in the vicinity of, but not well correlated with, tracers of urban emissions (Figures 5 and 6). For each ppbv of SO_2 present in the lower troposphere, ~4 μg m^{-3} of sulfate may ultimately be produced by oxidation (in the absence of losses due to dry deposition or precipitation). Thus the >3 ppbv of SO_2 remaining in the photochemically aged plumes encountered on these days represents >12 μg m^{-3} of additional, potential particulate sulfate.

[47] Throughout the data set, the fraction of measured nonrefractory particulate mass that is attributable to OM_{calc} was 0.56 ± 0.27; the remainder was almost entirely sulfate, ammonium, and water (at the measurement RH of 40%), since nitrate was only rarely above detection limits. There was a systematic trend in the relationship between the organic mass fraction and total submicron particle mass (Figure 8a). For submicron mass concentrations <15 μg m^{-3} (the U.S. annual mean national air

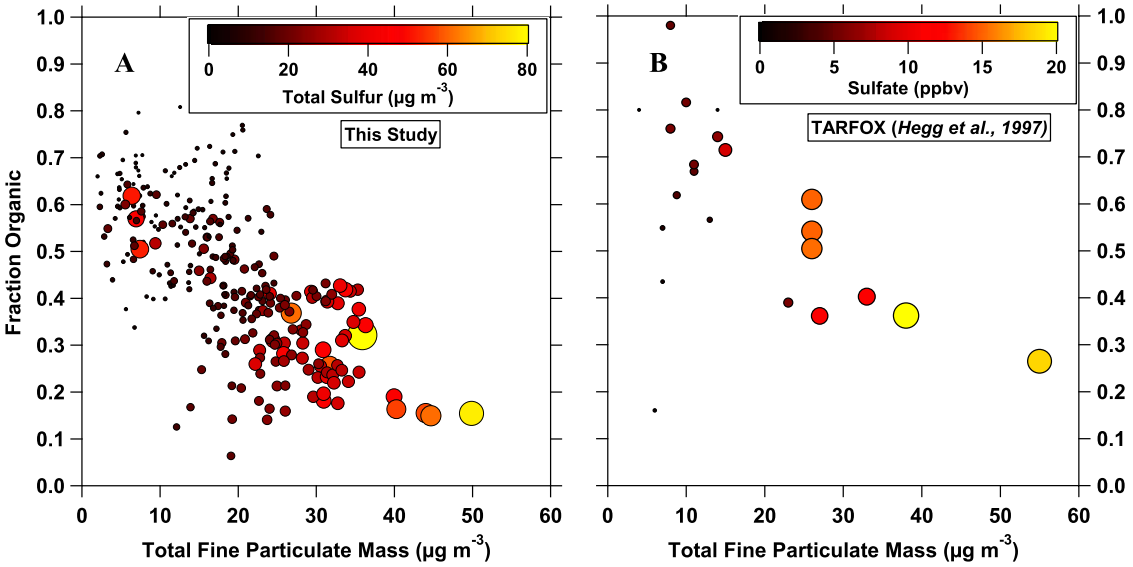

Figure 8. (a) Fraction of total particle mass that is due to OM_{calc} as a function of total particle mass, measured during the NEAQS/ITCT 2004 program. Symbols are color and size coded by total sulfur (SO_2 + particulate sulfate). (b) Fraction of total particle mass that is due to OM (estimated from measured particulate organic carbon) as a function of total particle mass measured during TARFOX, from *Hegg et al.* [1997, Table 3]. Symbols are color and size coded by particulate sulfate only (SO_2 was not reported). Several data points from Hegg et al. with low total mass loadings had indicated organic fractions >1 due to values near detection limits and are not plotted.

quality standard for mass of sub-2.5 μm particles), OM_{calc} typically represented 50% or more of the total submicron mass. For mass concentrations >15 μg m^{-3}, inorganic compounds, mostly sulfate and ammonium, dominated the submicron particulate mass. These high-mass cases were associated with high total sulfur (sulfate + SO_2), most of which originated from industrial and power generation facilities that combust coal.

[48] The data presented here are qualitatively consistent with those reported in the work of *Hegg et al.* [1997] and *Novakov et al.* [1997] from the TARFOX airborne measurements made over the mid-Atlantic coast of the U.S. (Figure 8b). In their analysis, Hegg et al. focused on the previously underappreciated importance of OM in particle chemistry and radiative properties. Our interpretation of these data is similar: for submicron particle loadings <15 μg m^{-3}, the organic fraction is frequently as important or more so than inorganic species. However, cases in the northeastern U.S. with submicron particle mass >15 μg m^{-3} were usually associated with elevated sulfate levels. Furthermore, since there was much additional potential sulfate mass present as unoxidized, gas-phase SO_2, then under multiday stagnation episodes (which were not encountered in the 2004 experiment) the importance of sulfate relative to OM_{calc} might increase even more.

[49] Our results indicate that on average, anthropogenic secondary OM_{calc} contributes the majority of the regional and urban submicron particle mass under typical, well ventilated conditions near anthropogenic sources, but that sulfate dominates submicron mass under conditions such as long-range transport that allow oxidation of substantial fractions of plume SO_2. In urban plumes, gas-phase VOCs oxidize to form secondary OM_{calc} with a time constant <1 d (part 1), while SO_2 oxidizes with an exponential time constant of 3–4 d at typical diurnally averaged OH concentrations of $\sim 3 \times 10^6$ molec cm^{-3} in this region and season [*Warneke et al.*, 2004]. Since VOCs and SO_2 are ubiquitous in the mixed urban/industrial regions of the northeastern U.S., the relative importance of each particulate mass source is dependent not only upon the emission strength, but also upon the time since emission relative to these oxidative timescales.

4.2. Gas-Phase SO_2 Oxidation Explains Observed Sulfate

[50] The interpretations in section 4.1 are dependent upon the assumption that SO_2 is photochemically oxidized. In the gas phase, the oxidation of SO_2 by OH is the rate-limiting step in the formation of particulate sulfate, with a reaction rate coefficient of $\sim 10^{-12}$ cm^3 molec^{-1} s^{-1} in the lower troposphere in the summer [*Seinfeld and Pandis*, 1998]. However, aqueous oxidation of SO_2 by O_3 and H_2O_2 in clouds may occur much more rapidly. In general, the loss rate of a reactive compound can be evaluated by examining the change in mixing ratio relative to a conserved, coemitted compound as a function of transport time. The production of particulate sulfate by oxidation of SO_2 can be analyzed using total plume sulfur as a conservative tracer (Figure 9). This assumption of sulfur conservation should be valid during transport in the free troposphere above the MBL and in the absence of precipitation scavenging, as was observed on the flights selected for this analysis. The observed increase in particulate sulfate relative to total plume sulfur is consistent with that expected from reaction of SO_2 with OH for a diurnally averaged OH concentration of $\sim 3 \times 10^6$ molec cm^{-3}. Thus the observed sulfate oxidation is mostly due to gas phase, rather than aqueous phase, processes in these cases. Note that the WP-3D flights

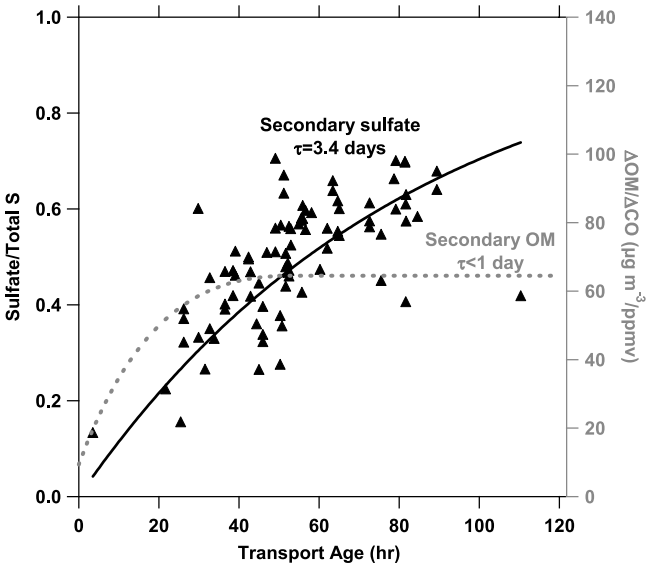

Figure 9. Ratio of sulfate to total sulfur (SO_2 + sulfate, left axis) and enhancement above background in particulate organic mass per unit enhancement in CO (dashed line, right axis, from *de Gouw et al.* [2007]), as a function of estimated plume age. Solid curve is an exponential least squares regression forced through y = 0 at a transport time of 0 h, since nearly all S is emitted as SO_2.

were biased toward transport cases with few clouds at the plume altitudes, so the observed photochemical oxidation of SO_2 in these data should not be generalized to describe all sulfur oxidation processes in this region and season.

4.3. Comparison With Other Observations

[51] *Bates et al.* [2005] provide a detailed evaluation of the relative contribution of OM and inorganic matter to submicron particle mass and to particle light scattering as determined from measurements made on the RHB during the NEAQS 2002 program in coastal waters off the northeastern U.S. Bates et al. concluded that OM on average contributed 41 (±9)% of submicron mass during conditions of southwesterly flow from the U.S. east coast urban corridor when the mass loadings were highest. Because of a more efficient mass scattering efficiency, OM was found to dominate visible light scattering measured at 55% RH during two pollution episodes downwind of major northeastern U.S. urban centers. These results are similar to those measured during TARFOX [*Hegg et al.*, 1997]. *Kleinman et al.* [2007], using airborne measurements predominantly over New England and adjacent waters, also found that organic mass dominated inorganic in all but plumes with total fine mass concentrations exceeding 20 μg m^{-3}, in which sulfate and associated ammonium dominated. These results contrast with those reported in the work of *Malm et al.* [2004], who reported that ~25% of sub-2.5 μm particle mass at mostly rural surface sites from the IMPROVE network in the northeastern U.S. in summer was OM, with sulfate and associated ammonium contributing >60% of the mass.

[52] The analysis presented here suggests some explanations for the differences between the long-term, inland IMPROVE observations showing sulfate dominance of fine particle mass and the RHB and TARFOX observations reporting OM dominance. During the NEAQS 2002 study, the RHB aerosol measurements sampled 18 m above the ocean surface, often within a shallow, stable MBL decoupled from flow aloft [*Angevine et al.*, 2006]. Most SO_2 from point sources is emitted from elevated stacks well above the surface to allow for improved ventilation and dispersion. While the RHB intercepted some concentrated SO_2 plumes from such point sources [e.g., *Bates et al.*, 2005, Figure 7], many others may have been present above the MBL. In fact, two isolated sulfate plumes originating from the Ohio River Valley were observed by aircraft at 1.3 and 1.7 km directly above the RHB during the 2002 study [*Canagaratna et al.*, 2007]. Urban sources from near-sea-level cities may have been sampled more readily on the RHB, thus biasing the shipboard observations. Rural IMPROVE network sites, on the other hand, in summertime are often in the well-mixed continental boundary layer, often cloud-topped, where particulate sulfate produced by gas and aqueous oxidation from near and distant SO_2 sources can be mixed to the surface and sampled.

[53] Perhaps more important than these differences in sampling altitude and mixing, however, is the observation in the work of *Bates et al.* [2005] that most urban air sampled aboard the RHB was transported over time periods of <24 h from coastal cities such as NYC and Boston. Given the time constant for production of secondary OM_{calc} from precursor VOCs of <1 d reported here and in the work of *de Gouw et al.* [2005] and *Sullivan et al.* [2006] as compared to the ~3–4 d photochemical oxidation time constant for SO_2 to produce sulfate, it is evident that observations made close to mixed urban/industrial sources are likely to contain more OM_{calc} relative to sulfate than are observations made after several days of oxidation. Similar arguments may be made for the TARFOX measurements made ~175 km downwind of the Washington D.C.–Baltimore urban area (~10 h with a 5 m s^{-1} wind). In some of the shipboard cases evaluated in the work of *Bates et al.* [2005, e.g., Figure 7], SO_2 mixing ratios ranged from ~1 to 5 ppbv, even outside of concentrated plumes, representing a potential sulfate source of ~4–20 μg m^{-3}. Such observations suggest that the importance of sulfate might be underestimated from measurements made under conditions of steady advection close to mixed urban/industrial sources. Indeed, *Quinn et al.* [2006], using measurements made aboard the RHB in the Gulf of Maine during the ICARTT 2004 mission, report that OM dominated submicron aerosol mass in plumes advected within 1 d from northeastern U.S. urban sources, but that the sulfate dominated in regional plumes more than 1 d old. Returning to the IMPROVE data set, we note most of the noncoastal IMPROVE sites lie west (generally upwind) of the major eastern U.S. urban sources, perhaps reducing the influence of these relatively fresh, OM-dominated urban plumes on the measured composition while increasing the influence of more aged sulfate-dominated plumes from the Ohio River Valley industrial region.

[54] Finally, we must emphasize these results apply to summertime conditions and only where photochemical processes dominate SO_2 oxidation. Under cloudier conditions, and especially in the winter season, SO_2 may be rapidly oxidized to sulfate by aqueous processing. In such conditions (and absent substantial production of OM by

aqueous processes) the importance of sulfate to the aerosol mass budget near emission sources could increase relative to the case of gas-phase oxidation alone. Furthermore, in cooler conditions, ammonium nitrate could play a more important role in the particulate mass budget, particularly near sources of ammonia.

4.4. Fluxes of OM_{calc} and Sulfate From the Eastern U.S.

[55] In part 1, a parameterization was developed that related secondary, anthropogenic OM_{calc} to anthropogenic CO emissions as a function of time since emission (Figure 9). This relationship was derived from analysis of the measurements of particulate VOC precursors, OM, and OM_{calc} derived from WSOC. The parameterization describes OM increases above background in anthropogenic plumes, but does not exclude a contribution to OM from enhanced oxidation of biogenic VOCs in these plumes. The parameterization was developed using data that explicitly excluded measurements made in plumes from biomass burning, and represents only the secondary production from VOC oxidation in plumes with elevated levels of anthropogenic CO. Production of CO from oxidation of biogenic VOCs in the plumes used to derive the CO-OM_{calc} relationship is negligible compared with the magnitude of the CO plume enhancements above background [*Griffin et al.*, 2007]. Assuming that this relationship derived by *de Gouw et al.* [2007] describes the production of OM_{calc} associated with all anthropogenic CO emissions in the northeastern U.S., we can use anthropogenic CO and SO_2 emission inventories to compare the potential production of secondary OM_{calc} in anthropogenic plumes with that of sulfate from SO_2. The EPA NEI 1999 V.3 inventory [*U.S. EPA*, 2003] gives total SO_2 emissions during the summer ozone season from the portion of the northeastern U.S. circled in Figure 1 of 4×10^6 kg d^{-1}, while anthropogenic CO emissions from this region total 3×10^7 kg d^{-1}. (Note that the CO emissions in this inventory are likely biased high [*Parrish et al.*, 2002]). The CO-OM_{calc} relationship reported by *de Gouw et al.* [2007] gives an ultimate yield of OM_{calc} from VOC oxidation of 0.03 kg of OM per kg of CO emitted, with an uncertainty of approximately a factor of 2. The production of OM_{calc} that is associated with anthropogenic CO emitted in the northeastern U.S. during the summer ozone season is then $0.4–1.8 \times 10^6$ kg d^{-1}. If all SO_2 emitted in the same region and time forms particulate ammonium bisulfate, the production of this compound is $\sim 8 \times 10^6$ kg d^{-1}. Thus, despite the higher-than-expected yields of OM_{calc} detailed in part 1, the potential production of inorganic particulate mass from SO_2 significantly exceeds the expected organic particulate mass from secondary production in anthropogenic plumes.

[56] The large potential particulate mass from SO_2 emissions implies that on average, the mass fraction of particulate sulfate compounds will be substantially larger than the secondary organic mass fraction associated with anthropogenic plumes during multiday stagnation episodes and following long-range transport from the eastern U.S. across the North Atlantic Ocean. The dominance of sulfate from controllable anthropogenic sources suggests that continued emphasis on reductions of SO_2 emissions from industrial and power generation point would be an effective strategy in reducing anthropogenic particulate mass concentrations at both regional and intercontinental scales. However, this evaluation does not include other significant sources of OM, including biomass burning (explicitly excluded from this data set), primary emissions, and regional secondary formation from biogenic VOCs that may occur outside of anthropogenic plumes. These sources may play increased roles when examining global budgets, rather than the plume enhancements above background which are the focus of this work.

[57] There are few relevant observations of particle composition far downwind from North America with which these calculations may be evaluated. Recently, *Lewis et al.* [2007] reported measurements of particle composition during the ICARTT time period over the North Atlantic Ocean near the Azores. Lewis et al. found slightly elevated but approximately equal mass concentrations of sulfate and organics (~ 1 μg m^3 each), averaged over time periods when low-altitude outflow of North American air (CO ~ 130 ppbv) was observed. It is unclear whether dilution during transport, or lack of urban/industrial influence, is responsible for the observed low concentrations of CO and aerosol mass. In either case, given the low concentrations reported by Lewis et al., it is difficult to compare their observed organic/sulfate ratios with those reported here and by *Quinn et al.* [2006] in much more concentrated plumes from known urban/industrial sources.

5. Conclusions

[58] Airborne observations of particle size distributions, particle composition, and gas-phase compounds were made downwind of urban and industrial sources near the northeastern coast of the U.S. during cloud-free transport in the summer. Nonrefractory submicron particle mass in the industrial/urban plumes was composed primarily of sulfate and associated ammonium, and OM. In most cases where submicron particle mass exceeded 15 μg m^{-3} (excluding biomass burning plumes), sulfate and associated ammonium contributed the majority of the mass. In the cases examined, this sulfate was produced from the SO_2 emitted from many modest-sized point and area sources associated with industrial and power generation facilities in and near the urbanized regions along the northeastern U.S. coast, with lesser contributions from upwind sources. Measured SO_2 decreased relative to total plume sulfur with a 3–4 d time constant consistent with gas-phase oxidation by OH.

[59] Because of these differing timescales for photochemical oxidation and production of secondary OM and sulfate, measurements made in urban plumes within 1 d transport of the source are likely to be dominated by OM in the summer in the absence of cloud processing. Measurements made in aged urban/industrial plumes in which SO_2 is abundant, a common occurrence in the northeastern U.S., are likely to dominated by sulfate and associated ammonium. Thus these differences in the timescales of photochemical production of OM_{calc} and particulate sulfate help explain the discrepancies in particle composition in this part of the U.S. that have been noted in the recent literature. Finally, when considering the long-range transport of particulate matter from the northeastern U.S., even accounting for higher-than-expected yields from OM formation [*de Gouw et al.*, 2005, 2007], the potential inorganic particulate mass represented by SO_2

emissions in this region significantly exceeds the potential OM associated with anthropogenic emissions of CO.

[60] **Acknowledgments.** This work was supported by the Climate Change and Air Quality Programs of NOAA. R. Peltier, A. Sullivan and R. Weber were supported by NOAA through contract A04OAR4310089. Support from the NOAA WP-3D flight crew is gratefully acknowledged. We are grateful to G. Chen of NASA Langley Research Center, who facilitated and moderated the DC-8/WP-3D instrument intercomparison, and to Brendan Matthew of Eastman Kodak Company for operating the PILS and AMS instruments on many flights.

References

Akimoto, H. (2003), Global air quality and pollution, *Science*, *302*, 1716–1719, doi:10.1126/science.1092666.

Angevine, W. M., J. E. Hare, C. W. Fairall, D. E. Wolfe, R. J. Hill, W. A. Brewer, and A. B. White (2006), Structure and formation of the highly stable marine boundary layer over the Gulf of Maine, *J. Geophys. Res.*, *111*, D23S22, doi:10.1029/2006JD007465.

Baron, P. A., and K. Willeke (2001), *Aerosol Measurement: Principles, Techniques, and Applications*, 2nd ed., John Wiley, New York.

Bates, T. S., D. J. Coffman, D. S. Covert, and P. K. Quinn (2002), Regional marine boundary layer aerosol size distributions in the Indian, Atlantic, and Pacific Oceans: A comparison of INDOEX measurements with ACE-1, ACE-2, and Aerosols99, *J. Geophys. Res.*, *107*(D18), 8026, doi:10.1029/2001JD001174.

Bates, T. S., P. K. Quinn, D. J. Coffman, J. E. Johnson, and A. M. Middlebrook (2005), Dominance of organic aerosol in the marine boundary layer over the Gulf of Maine during NEAQS 2002 and their role in aerosol light scattering, *J. Geophys. Res.*, *110*, D18202, doi:10.1029/2005JD005797.

Brock, C. A., F. Schröder, B. Kärcher, A. Petzold, R. Busen, and M. Fiebig (2000), Ultrafine particle size distributions measured in aircraft exhaust plumes, *J. Geophys. Res.*, *105*(D21), 26,555–26,567.

Canagaratna, M. R., et al. (2007), Chemical and microphysical characterization of ambient aerosol with the Aerodyne aerosol mass spectrometer, *Mass Spectrom. Rev.*, *26*, 185–222.

Clarke, A., et al. (2007), Biomass burning and pollution aerosol over North America: Organic components and their influence on spectral optical properties and humidification response, *J. Geophys. Res.*, *112*, D12S18, doi:10.1029/2006JD007777.

Daum, P. H., L. I. Kleinman, L. Newman, W. T. Luke, J. Weinstein-Lloyd, and C. M. Berkowitz (1996), Chemical and physical properties of plumes of anthropogenic pollutants transported over the North Atlantic during the North Atlantic Regional Experiment, *J. Geophys. Res.*, *101*(D22), 29,029–29,042.

de Gouw, J. A., C. Warneke, D. D. Parrish, J. S. Holloway, M. Trainer, and F. C. Fehsenfeld (2003), Emission sources and ocean uptake of acetonitrile (CH_3CN) in the atmosphere, *J. Geophys. Res.*, *108*(D11), 4329, doi:10.1029/2002JD002897.

de Gouw, J. A., et al. (2005), Budget of organic carbon in a polluted atmosphere: Results from the New England Air Quality Study in 2002, *J. Geophys. Res.*, *110*, D16305, doi:10.1029/2004JD005623.

de Gouw, J. A., et al. (2006), Volatile organic compounds composition of merged and aged forest fire plumes from Alaska and western Canada, *J. Geophys. Res.*, *111*, D10303, doi:10.1029/2005JD006175.

de Gouw, J. A., et al. (2007), Sources of particulate matter in the northeastern United States in summer: 1. Direct emissions and secondary formation of organic matter in urban plumes, *J. Geophys. Res.*, doi:10.1029/2007JD009243, in press.

Drewnick, F., J. T. Jayne, M. Canagaratna, D. R. Worsnop, and K. L. Demerjian (2004), Measurement of ambient aerosol composition during the PMTACS-NY 2001 using an aerosol mass spectrometer. Part II: Chemically speciated mass distributions, *Aerosol Sci. Technol.*, *38*, 104–117, doi:10.1080/02786820390229534.

Griffin, R. J., J. Chen, K. Carmody, S. Vutukuru, and D. Dabdub (2007), Contribution of gas phase oxidation of volatile organic compounds to atmospheric carbon monoxide levels in two areas of the United States, *J. Geophys. Res.*, *112*, D10S17, doi:10.1029/2006JD007602.

Hegg, D. A., J. Livingston, P. V. Hobbs, T. Novakov, and P. Russell (1997), Chemical apportionment of aerosol column optical depth off the mid-Atlantic coast of the United States, *J. Geophys. Res.*, *102*, 25,293–25,303.

Holloway, J. S., R. O. Jakoubek, D. D. Parrish, C. Gerbig, A. Volz-Thomas, S. Schmitgen, A. Fried, B. Wert, B. Henry, and J. R. Drummond (2000), Airborne intercomparison of vacuum ultraviolet fluorescence and tunable diode laser absorption measurements of tropospheric carbon monoxide, *J. Geophys. Res.*, *105*(D19), 24,251–24,261.

Huebert, B. J., et al. (2004), PELTI: Measuring the passing efficiency of an airborne low turbulence aerosol inlet, *Aerosol Sci. Technol.*, *38*, 803–826.

Jonsson, H. H., et al. (1995), Performance of a focused-cavity aerosol spectrometer for measurements in the stratosphere of particle size in the 0.06–2.0 μm diameter range, *J. Atmos. Oceanic Technol.*, *12*, 115–129.

Kanakidou, M., et al. (2005), Organic aerosol and global climate modeling: A review, *Atmos. Chem. Phys.*, *5*, 1053–1123, sref:1680-7324/acp/2005-5-1053.

Kleinman, L. I., et al. (2007), Aircraft observations of aerosol composition and ageing in New England and Mid-Atlantic States during the summer 2002 New England Air Quality Study field campaign, *J. Geophys. Res.*, *112*, D09310, doi:10.1029/2006JD007786.

Lewis, A. C., et al. (2007), Chemical composition observed over the mid-Atlantic and the detection of pollution signatures far from source regions, *J. Geophys. Res.*, *112*, D10S39, doi:10.1029/2006JD007584.

Li, Q. B., D. J. Jacob, R. M. Yantosca, J. W. Munger, and D. D. Parrish (2004), Export of NO_y from the North American boundary layer: Reconciling aircraft observations and global model budgets, *J. Geophys. Res.*, *109*, D02313, doi:10.1029/2003JD004086.

Mader, B. T., et al. (2003), Sampling methods used for the collection of particle-phase organic and elemental carbon during ACE-Asia, *Atmos. Environ.*, *37*, 1435–1449.

Malm, W. C., B. A. Schichtel, M. L. Pitchford, L. L. Ashbaugh, and R. A. Eldred (2004), Spatial and monthly trends in speciated fine particle concentration in the United States, *J. Geophys. Res.*, *109*, D03306, doi:10.1029/2003JD003739.

Markowski, G. R. (1988), Improving the Twomey algorithm for inversion of aerosol measurements data, *Aerosol Sci. Technol.*, *7*, 127–141.

McMurry, P., M. Shepherd, and J. Vickery (Eds.) (2004), *Particulate Matter Science for Policy Makers: A NARSTO Assessment*, Cambridge Univ. Press, Cambridge, U. K.

Neuman, J. A., et al. (2002), Fast-response airborne in situ measurements of HNO_3 during the Texas Air Quality Study, *J. Geophys. Res.*, *107*(D20), 4436, doi:10.1029/2001JD001437.

Neuman, J. A., et al. (2006), Reactive nitrogen transport and photochemistry in urban plumes over the North Atlantic Ocean, *J. Geophys. Res.*, *111*, D23S54, doi:10.1029/2005JD007010.

Novakov, T., D. A. Hegg, and P. V. Hobbs (1997), Airborne measurements of carbonaceous aerosols on the east coast of the United States, *J. Geophys. Res.*, *102*, 30,023–30,030.

Orsini, D. A., Y. Ma, A. Sullivan, B. Sierau, K. Baumann, and R. J. Weber (2003), Refinements to the particle-into-liquid sampler (PILS) for ground and airborne measurements of water soluble aerosol composition, *Atmos. Environ.*, *37*, 1243–1259.

Owen, R. C., O. R. Cooper, A. Stohl, and R. E. Honrath (2006), An analysis of the mechanisms of North American pollutant transport to the central North Atlantic lower free troposphere, *J. Geophys. Res.*, *111*, D23S58, doi:10.1029/2006JD007062.

Parrish, D. D., M. Trainer, D. Hereid, E. J. Williams, K. J. Olszyna, R. A. Harley, J. F. Meagher, and F. C. Fehsenfeld (2002), Decadal change in carbon monoxide to nitrogen oxide ratio in U.S. vehicular emissions, *J. Geophys. Res.*, *107*(D12), 4140, doi:10.1029/2001JD000720.

Parrish, D. D., et al. (2004), Fraction and composition of NO_y transported in air masses lofted from the North American continental boundary layer, *J. Geophys. Res.*, *109*, D09302, doi:10.1029/2003JD004226.

Peltier, R. E., A. P. Sullivan, R. J. Weber, C. A. Brock, A. G. Wollny, J. S. Holloway, J. A. de Gouw, and C. Warneke (2007), Fine aerosol bulk composition measured on WP-3D research aircraft in vicinity of the northeastern United States—Results from NEAQS, *Atmos. Chem. Phys.*, *7*, 3231–3247.

Quinn, P. K., and T. S. Bates (2005), Regional aerosol properties: Comparisons of boundary layer measurements from ACE 1, ACE 2, Aerosols99, INDOEX, ACE Asia, TARFOX, and NEAQS, *J. Geophys. Res.*, *110*, D14202, doi:10.1029/2004JD004755.

Quinn, P. K., et al. (2006), Impacts of sources and aging on submicrometer aerosol properties in the marine boundary layer across the Gulf of Maine, *J. Geophys. Res.*, *111*, D23S36, doi:10.1029/2006JD007582.

Ryerson, T. B., et al. (1998), Emissions lifetimes and ozone formation in power plant plumes, *J. Geophys. Res.*, *103*, 22,569–22,583.

Ryerson, T. B., E. J. Williams, and F. C. Fehsenfeld (2000), An efficient photolysis system for fast-response NO_2 measurements, *J. Geophys. Res.*, *105*, 26,447–26,461.

Santarpia, J. L., R. Li, and D. R. Collins (2004), Direct measurement of the hydration state of ambient aerosol populations, *J. Geophys. Res.*, *109*, D18209, doi:10.1029/2004JD004653.

Seinfeld, J. H., and S. N. Pandis (1998), *Atmospheric Chemistry and Physics: From Air Pollution to Climate Change*, Wiley-Intersci., New York.

Slusher, D. L., L. G. Huey, D. J. Tanner, F. M. Flocke, and J. M. Roberts (2004), A thermal dissociation–chemical ionization mass spectrometry (TD-CIMS) technique for the simultaneous measurement of peroxyacyl nitrates and dinitrogen pentoxide, *J. Geophys. Res.*, *109*, D19315, doi:10.1029/2004JD004670.

Stohl, A., M. Trainer, T. B. Ryerson, J. S. Holloway, and D. D. Parrish (2002), Export of NO_y from the North American boundary layer during 199 6 and 1997 North Atlantic Regional Experiments, *J. Geophys. Res.*, *107*(D11), 4131, doi:10.1029/2001JD000519.

Stohl, A., C. Forster, S. Eckhardt, N. Spichtinger, H. Huntrieser, J. Heland, H. Schlager, S. Wilhelm, F. Arnold, and O. Cooper (2003), A backward modeling study of intercontinental pollution transport using aircraft measurements, *J. Geophys. Res.*, *108*(D12), 4370, doi:10.1029/2002JD002862.

Sullivan, A. P., and R. J. Weber (2006a), Chemical characterization of the ambient organic aerosol soluble in water: 1. Isolation of hydrophobic and hydrophilic fractions with a XAD-8 resin, *J. Geophys. Res.*, *111*, D05314, doi:10.1029/2005JD006485.

Sullivan, A. P., and R. J. Weber (2006b), Chemical characterization of the ambient organic aerosol soluble in water: 2. Isolation of acid, neutral, and basic fractions by modified size-exclusion chromatography, *J. Geophys. Res.*, *111*, D05315, doi:10.1029/2005JD006486.

Sullivan, A. P., R. E. Peltier, C. A. Brock, J. A. de Gouw, J. S. Holloway, C. Warneke, A. G. Wollny, and R. J. Weber (2006), Airborne measurements of carbonaceous aerosol soluble in water over northeastern United States: Method development and an investigation into water-soluble organic carbon sources, *J. Geophys. Res.*, *111*, D23S46, doi:10.1029/2006JD007072.

Turpin, B. J., and H.-J. Lim (2001), Species contributions to PM2.5 mass concentrations: Revisiting common assumptions for estimating organic mass, *Aerosol Sci. Technol.*, *35*, 602–610, doi:10.1080/02786820119445.

United States Environmental Protection Agency (2003), National Emission Inventory documentation and data—Final version 3.0, Off. of Air Qual. Plann. and Stand., Research Triangle Park, N. C. (Available at http://www.epa.gov/ttn/chief/net/1999inventory.html)

Warneke, C., et al. (2004), Comparison of daytime and nighttime oxidation of biogenic and anthropogenic VOCs along the New England coast in summer during New England Air Quality Study 2002, *J. Geophys. Res.*, *109*, D10309, doi:10.1029/2003JD004424.

Warneke, C., S. Kato, J. A. de Gouw, P. D. Goldan, W. C. Kuster, M. Shao, E. R. Lovejoy, R. Fall, and F. C. Fehsenfeld (2005), Online volatile organic compound measurements using a newly developed proton-transfer ion-trap mass spectrometry instrument during New England Air Quality Study–Intercontinental Transport and Chemical Transformation, 2004. Performance, intercomparison, and compound identification, *Environ. Sci. Technol.*, *39*, 5390–5397, doi:10.1021/es050602o.

Wilson, J. C., B. Lafleur, H. Hilbert, W. Seebaugh, J. Fox, D. Gesler, C. Brock, B. Huebert, and J. Mullen (2004), Function and performance of a low turbulence inlet for sampling supermicron particles from aircraft platforms, *Aerosol Sci. Technol.*, *38*, 790–802.

E. L. Atlas, Rosenstiel School of Marine and Atmospheric Science, University of Miami, Miami, FL 33149, USA.

C. A. Brock, O. R. Cooper, J. A. de Gouw, F. C. Fehsenfeld, G. J. Frost, J. S. Holloway, G. Hübler, A. M. Middlebrook, J. A. Neuman, T. B. Ryerson, A. Stohl, M. K. Trainer, C. Warneke, and A. Wollny, Earth System Research Laboratory, NOAA, Boulder, CO 80305, USA. (charles.a.brock@noaa.gov)

R. E. Peltier and R. J. Weber, School of Earth and Atmospheric Sciences, Georgia Institute of Technology, Atlanta, GA 30332, USA.

A. P. Sullivan, Department of Atmospheric Science, Colorado State University, Fort Collins, CO 80523, USA.

J. C. Wilson, Department of Engineering, University of Denver, Denver, CO 80208, USA.